CHEMISTRY OF MATERIALS

ARTICLE

pubs.acs.org/cm

Formation of Sol−Gel-Derived TaO_xN_y Photocatalysts

Chiun-Teh Ho,[†] Ke-Bin Low,[‡] Panchatapa Jash,[§] Hongyan Shen,[§] Preston T. Snee,*[,§] and Randall J. Meyer*[,†]

[†]Department of Chemistry, [‡]Research Resource Center, and [§]Department of Chemical Engineering, University of Illinois at Chicago, Chicago, Illinois 60607, United States

Supporting Information

ABSTRACT: Tantalum oxynitride (TaON) is a visible photocatalyst (λ < 520 nm) that has been investigated for green energy applications, specifically, the solar production of hydrogen gas. Metal oxynitrides are often generated by the ammonolysis of metal oxides at very high temperatures. We have investigated an alternative synthetic procedure to produce gram-scale quantities of photocatalytically active TaO_xN_y materials using room-temperature sol−gel chemistry. X-ray photoelectron spectroscopy (XPS) results confirm that nitrogen was incorporated into materials with a Ta_2O_5 crystal structure. Optical characterization reveals that sol−gel-synthesized TaO_xN_y has a 2.3 eV bandgap, in agreement with bulk TaON. Furthermore, photoluminescence experiments reveal that two distinct material systems are being created during the initial sol phase of the synthesis: one species is primarily metal oxide, while the other is a N-doped species. This observation may lead to synthetic methods that improve the doping content of sol−gel-derived materials.

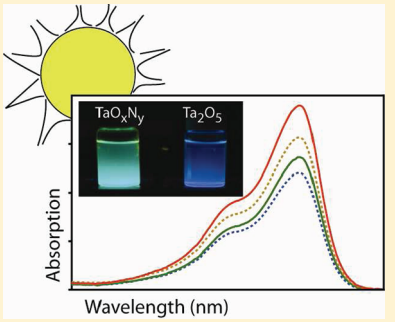

KEYWORDS: photocatalyst, tantalum oxynitride, solar energy, oxynitride, sol−gel

INTRODUCTION

The generation of alternative and renewable energy sources is a significant challenge that is essential toward sustaining long-term economic stability. Solar energy collection and H_2 production using water splitting photocatalysts are important processes to achieve our energy goals. Metal oxide semiconductors are highly effective in this regard;[1−3] however, these materials have very large bandgaps that preclude effective solar energy harvesting.[4] Domen et al. have shown that oxynitride materials have the appropriate redox potentials coupled to low bandgaps that allow for solar energy harvesting.[5−8] The strategy for selection of metal oxynitrides is based on the fact that nitrogen has an atomic valence bond-forming orbital (2p) with a higher oxidation potential than oxygen. At the same time, the metal-centered conduction band is unaltered and strong enough to reduce $H^+_{(aq)}$. Several methods have been developed to dope nitrogen into semiconductor oxides to examine band-gap engineering for energy-related applications.

Previously, our group studied the colloidal synthesis of Ta_3N_5 nanoparticles;[9] although successful, problems were encountered with the oxidation of tantalum during the synthesis resulted in very low reaction yields. As such, our developments are based on the synthesis of the oxynitride directly, because this material is also a useful photocatalyst, although it has a higher bandgap than Ta_3N_5. Ito et al.[10] showed that TaON is ∼20 times more active as a visible-light-activated photocatalyst for the oxidation of methanol, compared to the ubiquitous TiO_2 (Degussa P25) catalyst. The TaON samples in this study were created by nitriding the oxide at a high temperature (850 °C) for 15 h under a flow of nitrogen gas bubbled through aqueous ammonium hydroxide. We have sought to develop a simpler and less-expensive method for the creation of TaON that avoids high-temperature nitriding using ammonia gas.[11,12] We demonstrate that it is, in fact, possible to create photocatalytically active TaO_xN_y using an inexpensive, low-temperature sol−gel method.

The sol−gel process[13,14] is essentially an inorganic polymerization reaction and is useful for the preparation of inorganic materials such as glasses and ceramics.[15−19] The first step generally begins with the hydrolysis of a monomeric metal or semimetal alkoxide precursor $M(OR)_n$, where M represents a network-forming element such as Al, B, Si, Ta, Ti, Zr, etc., and R is typically an unsaturated alkyl group, in a mixed water/alcohol solution. The resulting sol is set to a gel with the addition of an acid or base catalyst, although both hydrolysis and condensation reactions occur simultaneously once the hydrolysis reaction has been initiated. The solvent and low-molecular-weight byproducts such as alcohol and water are then removed from the system. This causes a significant level of shrinkage of the gel.[20] The structure and morphology of the resulting network is strongly dependent on the nature of the catalyst, the presence of surfactants, and the pH of the reaction. In addition, the size of the alkoxy group can also influence the hydrolysis and condensation reactions through steric or leaving group stability effects.

In 2003, Burda[21,22] developed a procedure using sol−gel chemistry to synthesize $TiO_{2-x}N_x$ materials; nitrogen was doped into titania at a level as high as 8%. $TiO_{2-x}N_x$ was synthesized at room temperature by employing the direct nitridation of anatase TiO_2 nanostructures with triethylamine. The synthesized $TiO_{2-x}N_x$

Received: May 25, 2011
Revised: September 3, 2011
Published: October 07, 2011

materials are photocatalytically active, with absorbance that extends into the visible region (up to 550 nm). A follow-up report from the same group demonstrated an alternative procedure to synthesize N-doped TiO_2.[22] A gel of agglomerated TiO_2 nanoparticles was exposed to an excess of triethylamine, forming a $TiO_{2-x}N_x$ nanocolloid within seconds, as evident from the heat that is released at the same time. The dried mixture forms orange crystallites. Further studies have demonstrated that hydrazine and ethylenediamine are effective organic sources of nitrogen for doping metal oxides.[23,24]

Although the sol−gel process developed by Gole and Burda has demonstrated success in creating N-doped TiO_2 and CeO_2, this technique has not been applied to other materials (such as Ta_2O_5). In this report, we describe a simple sol−gel method that leads to the formation of N-doped, stable, and environmentally benign TaO_xN_y materials that are potential photocatalysts for water splitting; these materials are shown to be photocatalytically active for wastewater remediation in this report.

EXPERIMENTAL SECTION

A solution of 0.90 mL (3.46 mmoL) of tantalum(V) ethoxide ($Ta(OC_2H_5)_5$, 99.99+%, Strem) and 5.13 mL of ethylenediamine (99%, Fluka, vacuum-distilled) were added to 40.0 mL of 1-butanol (anhydrous, Aldrich). The solution was refluxed while stirring for 72 h, forming a yellow-colored solution. This solution was divided into four vials; the sol was set was set with acetic acid, as discussed below, or could be stored for further processing and optical characterization. The solution is stable for weeks under ambient conditions.

To form a gel, 3.35 mL of glacial acetic acid (99.8%, Sigma−Aldrich) was added slowly into a vial; the resulting solution was hydrolyzed via a dropwise addition of 3.35 mL of 18 MΩ distilled water. Then, 3.35 mL of a 1 M KOH solution was added. Finally, the resulting flocculants were centrifuged and washed with ethanol and distilled water several times and dried under vacuum for 24 h. The resultant dry light yellow powders were characterized as prepared or after sintering at various high temperatures under a nitrogen atmosphere. A control sample of Ta_2O_5 was prepared using methodology identical to that previously described, without the addition of ethylenediamine.

Characterization. The resulting TaO_xN_y products were characterized optically (ultraviolet−visible light (UV−vis) spectroscopy, using a Cary 300 system; infrared (IR) spectroscopy, using a JASCO Model FT/IR-4100 system; and photoluminescence, using a Horiba Jobin−Yvon Model Fluorlog-3 spectrofluorometer), via X-ray photoelectron spectroscopy (XPS) (Kratos Model AXIS-165 at 15 kV, 10 mA; an adventitious C 1s feature at 284.8 eV was used to calibrate the spectra), via X-ray diffraction (XRD) (Siemens Model D-5000), and using Brunauer−Emmett−Teller (BET) analysis to calculate the surface area (Micromeritics Model ASAP 202 surface area and porosity analyzer). The custom-designed Fluorolog-3 spectrofluorimeter follows a classical configuration, using a xenon arc lamp excitation source, excitation and emission double monochromators, an excitation reference photodiode, and a thermoelectrically cooled photomultiplier tube (Products for Research) for detection. Samples were held under ambient conditions for these measurements. Photocatalytic activity was measured by monitoring the bleach of aqueous methylene blue (Acros, certified) with and without the presence of 0.1 g of as-prepared TaON while stirring; the tripled 355-nm output of a Nd:YAG laser (Powerlight, Continuum) was used as the excitation source.

The nitrogen content of TaO_xN_y products as a function of sintering temperature was investigated by XPS; the crystallinity was probed with XRD. Previous work examining $TiO_{2-x}N_x$ materials demonstrated that the nitrogen content significantly affects the electronic structure,[25,26] which, in turn, alters the visible-light absorbance and photocatalytic activity. Thus, characterizing the N-dopant level is important to evaluate the efficacy of the materials for industrial application.

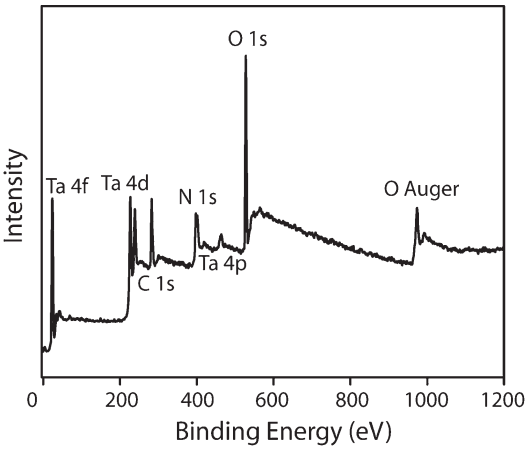

Figure 1. XPS survey of as-prepared (unsintered) TaO_xN_y made via a sol−gel method.

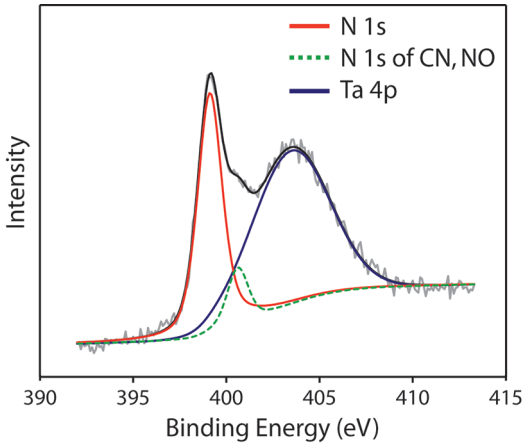

Figure 2. XPS spectrum of as-prepared (unsintered) TaO_xN_y material in the N 1s region. Black line is the fit to the raw data (gray line) summed from individual components (colored lines).

RESULTS AND DISCUSSION

XPS Spectra. The changes in the nitrogen content and crystallinity of TaO_xN_y powders after sintering at variable temperatures were investigated by XPS and XRD, respectively. Figure 1 shows the XPS survey spectrum of the as-prepared (unsintered) TaO_xN_y material. The spectrum shows typical Ta^{5+} features; furthermore, no Ta^0 metal peak was observed in this or any other sample. Figure 2 shows the XPS spectrum of the as-prepared (unsintered) TaO_xN_y material in the N 1s region; a sharp N 1s peak at 399.1 eV is present in the data and a small shoulder observed at 400.9 eV. Compared to previous reports and our own results after sintering, the 400.9 eV peak must originate from organic residues[27] on the surface or, more likely, embedded into the solid-state material.[28] Similarly, the lower-energy feature may be due to N occupying an interstitial site in the Ta_2O_5 matrix; similar results have been observed in N-doped TiO_2.[29] Most interesting is the fact that a metal-coordinated nitrogen feature is observable without the need for Ar^+ etching.[29] Furthermore, Ar^+ sputtering of the unsintered sample reveals a 395.0 eV feature

dx.doi.org/10.1021/cm2014847 |Chem. Mater. 2011, 23, 4721–4725

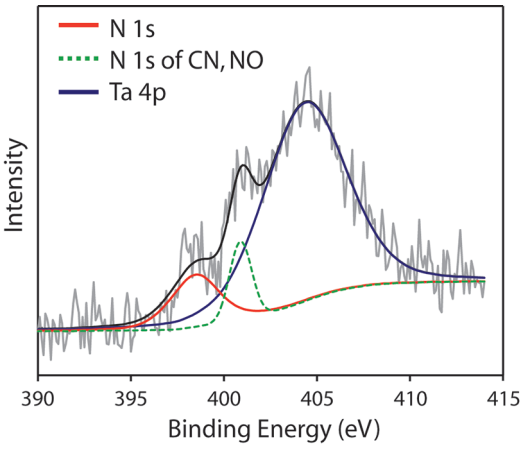

Figure 3. XPS spectrum of TaO_xN_y in the N 1s region after sintering for 1 h at 1000 K. Black line is the fit to the raw data (gray line) summed from individual components (colored lines).

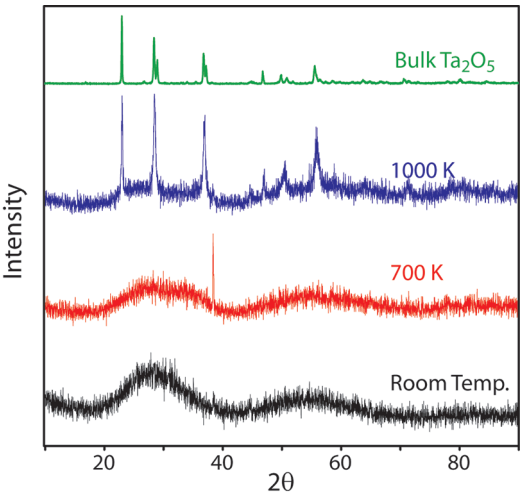

Figure 4. XRD spectra of TaO_xN_y powders, as a function of the post-annealing temperature. Black line is the spectrum of as-prepared powders. Red line is the spectrum of the materials sintered at 700 K for 1 h under an N_2 atmosphere (the feature at ~40° is likely an artifact). Blue line is the spectrum of materials sintered at 1000 K for 1 h under an N_2 atmosphere, which is well-matched to bulk tantalum oxide (green line).[9]

that is consistent with the 395.4 eV N 1s transition observed in bulk powder TaON synthesized by Maeda and co-workers[9] (see Figure S1 in the Supporting Information).

Figure 3 shows the XPS spectrum in the N 1s region of TaO_xN_y materials sintered at 1000 K under a N_2 atmosphere. The ~399 eV Ta−N peak in the as-prepared material red-shifts to 398.6 eV and decreases in intensity. Compared to previous results, the red-shifted 398.6 eV is similar to the 395.4 eV N 1s feature from bulk crystalline powder TaON[9] and indicates a greater degree of Ta−N bonding.[30] As a result, we attribute this feature to interstitial N-doping, which gains more Ta−N character with annealing. Oddly, Ar^+ sputtering of this annealed sample does not reveal an oxynitride ~395 eV feature, as observed in the as-prepared material (see Figure S2 of the Supporting Information).

The Ta 4f transition was used to normalize XPS data to calculate the atomic percent concentrations of Ta and N, as a function of sintering temperature; the N 1s peak at ~399 eV is used for this calculation. Initially, the Ta:N ratio is 2:3 (40.8% to 59.2%), which increases to 2:1 (68.8% to 31.2%) after sintering the material at 1000 K. This is consistent with the data presented in Figures 2 and 3, where the N 1s (shift to 398.6 eV) transition is weaker after 1000 K sintering. Burda's group also observed a similar N loss in doped TiO_2 materials after sintering under either air or N_2 atmospheres.[24] The peak of N at 400.9 eV does not change significantly before (19.2%) and after (21.1%) sintering. After sintering, the yellow powders turn black; we attribute this to the presence of carbon in the sintered material, which is corroborated with Fourier transform infrared (FTIR) data (see the Supporting Information). The carbon is likely bound to nitrogen, giving rise to the 400.9 eV feature in the sintered and unsintered XPS spectra. As such, we attribute the 400.9 eV feature to the presence of nitrogen-containing organic species.

XRD Results. The XRD spectra of TaO_xN_y materials as a function of sintering temperature are shown in Figure 4. The TaO_xN_y powders are amorphous after sintering at temperatures below 700 K under a N_2 atmosphere, while the XRD patterns of TaO_xN_y sintered at 1000 K correspond to Ta_2O_5. Diffraction peaks indicating the presence of crystalline TaON are not observed. These results are consistent with studies on N-doped titanium dioxide powders that develop long-range crystallinity (TiO_2 anatase) at temperatures above 673 K.[24] While a significant amount of nitrogen incorporation is indicated from XPS results, the XRD data demonstrate that nitrogen must be incorporated into vacancies, interstitial, and defect sites in the Ta_2O_5 structure.

Absorption and Emission. The absorption and PLE spectrum of the TaO_xN_y sol (before addition of acetic acid) are shown in Figure 5A. The spectrum show strong absorption features at >330 nm with a weak tail extending from 400 nm to 500 nm. The emission spectrum was also measured as shown in Figure 5B. Surprisingly, when TaO_xN_y is excited at 320 nm, two different emission features are observed: one at 352 nm (3.53 eV) and another at 530 nm (2.33 eV). As seen in the inset of Figure 5B, the TaO_xN_y sample has a visible green emission in contrast to the weak blue emission of a pure Ta_2O_5 sol (prepared without addition of ethylenediamine). The spectrum indicates that two distinctly different materials simultaneously exist in solution. The 530 nm (2.33 eV) feature is close to the bandgap of bulk TaON (2.4 eV). It is tempting to assign stoichiometrically pure TaON as being responsible for this observation; however, we believe that a N-doped TaO_xN_y sol with red-shifted defect-state emission is more likely responsible, because of the lack of TaON patterns in the XRD data and the width of the emission feature. As discussed below, the defect state may be due to reduced Ta metal centers that form as a result of vacancies in the metal coordination sphere. Also note that the energy of the 352 nm (3.5 eV) emission feature is less than the bulk bandgap of Ta_2O_5 (3.9 eV); the only feasible explanation for this observation is emission from defects in a Ta_2O_5 sol.

Photoluminescence Excitation (PLE). To examine the electronic structure of the TaO_xN_y sol, the PLE spectrum is recorded by monitoring the intensity of emission at 530 nm, as a function of excitation wavelength, as shown in the inset of Figure 5A. The results reflect the absorption spectrum of the material responsible for the 530-nm emission of the TaO_xN_y sol. This PLE spectrum does not have the structure of an organic chromophore that could have formed as a side product; however, the data are also inconsistent with a low-energy-bandgap doped semiconductor. Figure 6 shows the PLE spectrum as a function of excitation energy; the data were fit to multiple Gaussian functions that reveal the existence of possibly two singular sub-band-gap states

dx.doi.org/10.1021/cm2014847 |Chem. Mater. 2011, 23, 4721–4725

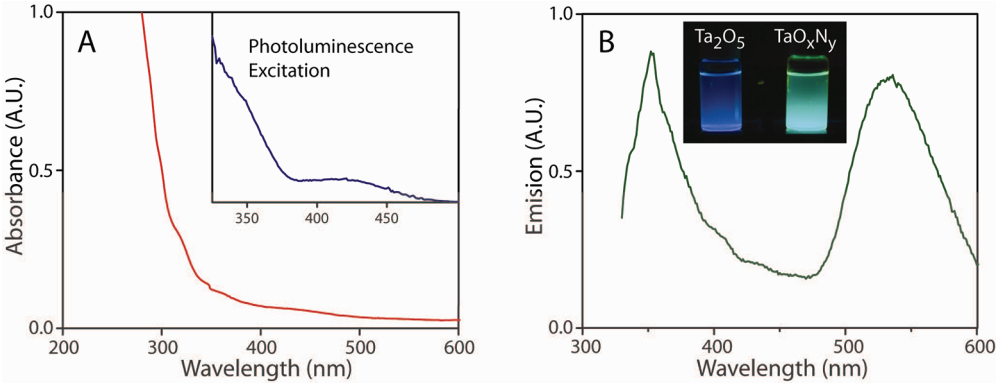

Figure 5. (A) Absorption spectrum of the TaO_xN_y sol after 3 days refluxing in solution (before setting the sol with acidic water). Inset shows the PLE spectrum monitoring the emission at 530 nm. (B) Emission spectrum of TaO_xN_y sol after 3 days refluxing in solution (before setting the sol with acid) displays two prominent features. Inset demonstrates the visible emission of a pure Ta_2O_5 sol made without the use of an amine precursor, and a TaO_xN_y sample.

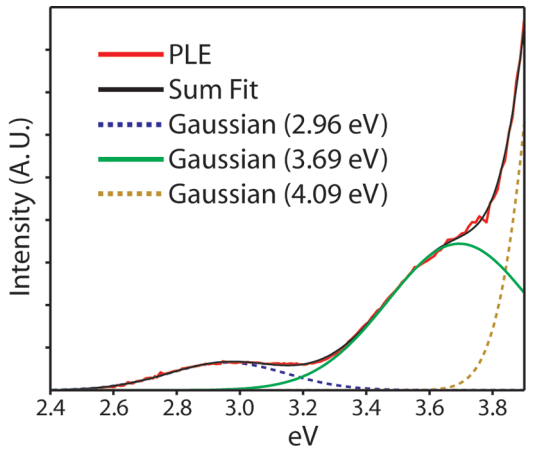

Figure 6. Energy-dependent decomposition of the PLE spectrum of Figure 5A (inset) reveals two Gaussian-distributed states below the pure oxide bandgap of 3.9 eV. These data suggest that sub-band-gap semiconductor-like states are not responsible for the red-shift of N-doped TaO_xN_y sols.

centered at 2.96 and 3.69 eV. As recently shown by Kuznetsov et al.,[31] such well-defined sub-band-gap states may form due to vacancies in oxidized metal coordination sphere (or "color centers")[31,32] that result indirectly from the presence of dopants, as opposed to the formation of doped sub-band-gap states. Regardless of the nature of the sub-band-gap states, the dual luminescence of the sol material shown in Figure 5B demonstrates that two distinct species are being created during the initial sol phase of the synthesis: a pure oxide and a N-doped material. This offers the possibility that the effects of nitrogen doping can be increased if the mechanisms for forming these two species are determined, because perhaps the chemistry can be altered to strongly favor the one material over the other.

Photocatalytic Activity. To characterize sol–gel-derived TaO_xN_y materials as possible photocatalysts, we have measured the surface area of the as-prepared TaON and TaON sintered at 1000 K, and we have examined the utility of TaON gels for light-driven aqueous organic waste remediation. The sintering of the material was found to have a significant effect on the surface area, reducing it from 118 ± 1 m^2/g for the as-prepared material to 0.57 ± 0.01 m^2/g upon annealing at 1000 K. We believe that this may be explained by the reduction of organic species into carbon at the surface of the black sintered powders. The as-prepared TaON gel, despite its amorphous crystallinity, was found to assist the photodegradation of methylene blue in water catalytically, which is an often-employed model for wastewater remediation. The photocatalytic activity may also be increased by the addition of a metal co-catalyst, as was demonstrated in recent reports.[33,34]

CONCLUSION

Previous work has demonstrated that N-doped TiO_2 can be synthesized via a sol–gel method. A similar approach has been applied to create N-doped Ta_2O_5 using tantalum alkoxide and ethylenediamine precursors. From the XPS results, N atoms are successfully incorporated into a Ta_2O_5 framework to form an amorphous TaO_xN_y material that is photocatalytically active. The results also show some nitrogen is bound to organic species. Post-sintering at 1000 K in a N_2 atmosphere helps to improve the crystallinity of the materials; however, the nitrogen content decreases and the presence of TaON is not observed.

Two emission features in the fluorescence spectrum demonstrated the successful synthesis of TaO_xN_y that exists simultaneously with Ta_2O_5 materials; examination of the PLE data suggest that the optical properties of the doped material may be due to reduced metal "color centers". This offers the possibility of enhancing the N-doping levels if the mechanism for forming both species can be determined. Future work will examine the catalytic efficiency of the sol–gel-derived materials for a variety of applications.

ASSOCIATED CONTENT

Supporting Information. XPS spectra of materials before and after Ar^+ etching, TEM micrographs of TaON sols, and FTIR and photocatalytic performance data. (PDF) This material is available free of charge via the Internet at http://pubs.acs.org.

AUTHOR INFORMATION

Corresponding Author

*E-mail addresses: sneep@uic.edu (P.T.S.), rjm@uic.edu (R.J.M.).

ACKNOWLEDGMENT

We thank Profs. Kazunari Domen and Kazuhiko Maeda for a sample of TaON powder and Prof. Michael Trenary for

assistance with experiments. Also, Ali Jawaid and Jingjing Liu for help with characterization of materials. This work was supported by the UIC Chancellor's Discovery Fund, the University of Illinois at Chicago (to PTS and R.J.M), and a PRF award (50859-ND10) to P.T.S from the ACS.

REFERENCES

(1) Ni, M.; Leung, M. K. H.; Leung, D. Y. C.; Sumathy, K. *Renew. Sust. Energy Rev.* **2007**, *11*, 401.
(2) Hameed, A.; Gondal, M. A. *J. Mol. Catal. A—Chem.* **2004**, *219*, 109.
(3) Yamakata, A.; Ishibashi, T.; Onishi, H. *J. Mol. Catal. A—Chem.* **2003**, *199*, 85.
(4) Chen, X.; Mao, S. S. *Chem. Rev.* **2007**, *107*, 2891.
(5) Maeda, K.; Domen, K. *J. Phys. Chem. C* **2007**, *111*, 7851.
(6) Takata, T.; Hitoki, G.; Kondo, J. N.; Hara, M.; Kobayashi, H.; Domen, K. *Res. Chem. Intermed.* **2007**, *33*, 13.
(7) Hitoki, G.; Takata, T.; Kondo, J. N.; Hara, M.; Kobayashi, H.; Domen, K. *Chem. Commun.* **2002**, 1698.
(8) Hara, M.; Takata, T.; Kondo, J. N.; Domen, K. *Catal. Today* **2004**, *90*, 313.
(9) Ho, C.-T.; Low, K.-B.; Klie, R. F.; Maeda, K.; Domen, K.; Meyer, R. J.; Snee, P. T. *J. Phys. Chem. C* **2011**, *115*, 647.
(10) Ito, S.; Thampi, K. R.; Comte, P.; Liska, P.; Gratzel, M. *Chem. Commun.* **2005**, 268.
(11) Murase, T.; Irie, H.; Hashimoto, K. *J. Phys. Chem. B* **2004**, *108*, 15803.
(12) Lu, D. L.; Hitoki, G.; Katou, E.; Kondo, J. N.; Hara, M.; Domen, K. *Chem. Mater.* **2004**, *16*, 1603.
(13) Wen, J. Y.; Wilkes, G. L. *Chem. Mater.* **1996**, *8*, 1667.
(14) Sanchez, C.; Ribot, F. *New J. Chem.* **1994**, *18*, 1007.
(15) Sakka, S.; Kamiya, K. *J. Non-Cryst. Solids* **1980**, *42*, 403.
(16) Sakka, S. *J. Non-Cryst. Solids* **1985**, *73*, 651.
(17) Yoldas, B. E. *J. Non-Cryst. Solids* **1984**, *63*, 145.
(18) Ulrich, D. R. *CHEMTECH* **1988**, *18*, 242.
(19) Brinker, C. J.; Scherer, G. W. *Sol—Gel Science, The Physics and Chemistry of Sol-Gel Processing*; Academic Press: Boston, 1990.
(20) Yoldas, B. E. J. *Mater. Sci.* **1986**, *21*, 1087.
(21) Burda, C.; Lou, Y. B.; Chen, X. B.; Samia, A. C. S.; Stout, J.; Gole, J. L. *Nano Lett.* **2003**, *3*, 1049.
(22) Gole, J. L.; Stout, J. D.; Burda, C.; Lou, Y. B.; Chen, X. B. *J. Phys. Chem. B* **2004**, *108*, 1230.
(23) Mao, C. J.; Zhao, Y. X.; Qiu, X. F.; Zhu, J. J.; Burda, C. *Phys. Chem. Chem. Phys.* **2008**, *10*, 5633.
(24) Zhao, Y. X.; Qiu, X. F.; Burda, C. *Chem. Mater.* **2008**, *20*, 2629.
(25) Asahi, R.; Morikawa, T.; Ohwaki, T.; Aoki, K.; Taga, Y. *Science* **2001**, *293*, 269.
(26) Chen, X. B.; Lou, Y. B.; Samia, A. C. S.; Burda, C.; Gole, J. L. *Adv. Funct. Mater.* **2005**, *15*, 41.
(27) Jansen, R. J. J.; Vanbekkum, H. *Carbon* **1995**, *33*, 1021.
(28) Diwald, O.; Thompson, T. L.; Zubkov, T.; Goralski, E. G.; Walck, S. D.; Yates, J. T. *J. Phys. Chem. B* **2004**, *108*, 6004.
(29) Rengifo-Herrera, J. A.; Pierzchala, K.; Sienkiewicz, A.; Forro, L.; Kiwi, J.; Moser, J. E.; Pulgarin, C. *J. Phys. Chem. C* **2010**, *114*, 2717.
(30) Chun, W. J.; Ishikawa, A.; Fujisawa, H.; Takata, T.; Kondo, J. N.; Hara, M.; Kawai, M.; Matsumoto, Y.; Domen, K. *J. Phys. Chem. B* **2003**, *107*, 1798.
(31) Kuznetsov, V. N.; Serpone, N. *J. Phys. Chem. B* **2006**, *110*, 25203.
(32) Serpone, N. *J. Phys. Chem. B* **2006**, *110*, 24287.
(33) Hsieh, J. H.; Chang, C. C.; Li, C.; Liu, S. J.; Chang, Y. K. *Surf. Coat. Technol.* **2010**, *205*, S337.
(34) Maeda, K.; Terashima, H.; Kase, K.; Domen, K. *Appl. Catal., A* **2009**, *357*, 206.